Neuropathological characterization of camel prion disease

Rosalia Bruno[1]*, Baaissa Babelhadj [2,3], Laura Pirisinu[1], Geraldina Riccardi[1], Barbara Chiappini[1], Romolo Nonno[1], Umberto Agrimi[1], Gabriele Vaccari[1] and Michele Angelo Di Bari[1]

[1] *Department of Food Safety, Nutrition and Veterinary Public Health; Italian National Institute of Health; Rome, Italy.*
[2] *Ecole Normale Superieure Ouargla, Algeria*
[3] *Laboratoire de Protection des Écosystèmes en Zones Arides et Semi Arides University Kasdi Merbah Ouargla, Algeria.*

*Presenting author Mail address: rosalia.bruno@iss.it

INTRODUCTION

Camel prion disease (CPrD) of dromedary camel (Camelus dromedarius), belongs to a group of fatal neurodegenerative pathologies affecting animals and humans called prion diseases (Babelhadj et al., 2018). CPrD was first observed in Algeria, in 2016 (Babelhadj et al., 2018) and later identified also in Tunisia in 2019 (OIE, 2019). The geographical distribution and prevalence of CPrD in the camel population worldwide are unknown. Observations from Algeria indicate a prevalence of 3.1% in animals brought to the abattoir of Ouargla (Babelhadj et al., 2018). These data suggest the high prevalence of disease and the need for further investigation.

The present study aimed to obtain a detailed neuropathological description of the CPrD, in terms of both spongiform change and PrP^{Sc} accumulation. It also aimed to provide a descriptive baseline to define the best brain areas to be used for diagnostic investigations and to explore the phenotypical variability of the disease.

MATERIALS AND METHODS

Samples - The brains of nine symptomatic CPrD-confirmed dromedaries, along with one CPrD-negative animal, were analyzed. Individual details of the dromedaries used in this study are in Table 1.

Neuropathological analysis - According to standard histopathological procedures, brain tissues were trimmed to standard levels and processed. Neuroanatomical structures were identified with reference to anatomical studies of dromedary camel brain (Abedellaah et al., 2015; Zhaohui et al., 2011). Neuroanatomical distribution and deposition pattern of PrP^{Sc} were evaluated respectively by both IHC and Pet-blot (Babelhadj et al., 2018).

Evaluation of spongiform change and PrP^{Sc} deposits (L42 mAb) was performed blind to the ID identification. Each brain region was scored for vacuolation and PrP^{Sc} immunolabeling using the following severity scale: 0, absence; 1, minimal; 2, slight; 3, moderate; 4, marked; 5, intense.

Dromedary ID	Data of collection	Clinical symptoms	Age (years)	Sex	PRNP genotype	Diagnosis	Brain areas available
#3*	2016	Yes	10	F	n.a.	+	Hemi-encephalon (no cerebell.)
#4*	2016	Yes	11	F	WT	+#	Hemi-encephalon
#5*	2016	No	14	F	n.a.	-	Hemi-encephalon
#8*	2017	Yes	13	F	WT	+#	Hemi-encephalon**
#10	2019	Yes	11	F	WT	+	Occipital ctx
#11	2019	Yes	10	F	WT	+	Occipital ctx, hippocampus, midbrain, caudal brainstem, cerebellum
#18	2020	Yes	14	F	WT	+	Cerebellum
#61	2020	Yes	14	F	WT	+	Pons, cerebellum
#54	2021	Yes	9	F	WT	+	Pons
#56	2021	Yes	9	F	WT	+	Pons

Table 1. Details on dromedaries examined in this work
* Previously included in Babelhadj et al., 2018.

RESULTS

Histopathological and immunohistochemical (IHC) analyses highlighted a specific and homogeneous neuroanatomical distribution of spongiform change and PrP^{Sc} deposition in all CPrD cases (Figure 1).

Distribution of spongiform change in the brain

Spongiform change was mainly detected in subcortical areas and brainstem, while it was rarely observed in the cortices (Figure 1 and 2). Interestingly, we found that vacuoles in subcortical areas were mostly observed in neuropil and neuronal perikarya, while, in the cortices, they were mainly present in the neuropil (Figure 2). We observed that the anterior portion of cerebral cortex was more affected by spongiosis than the mid and posterior ones. The evaluation of density and distribution of spongiform change highlights the wide neuropathological damage involving the whole brain (Figure 1). No spongiosis was seen in the CPrD-negative brain.

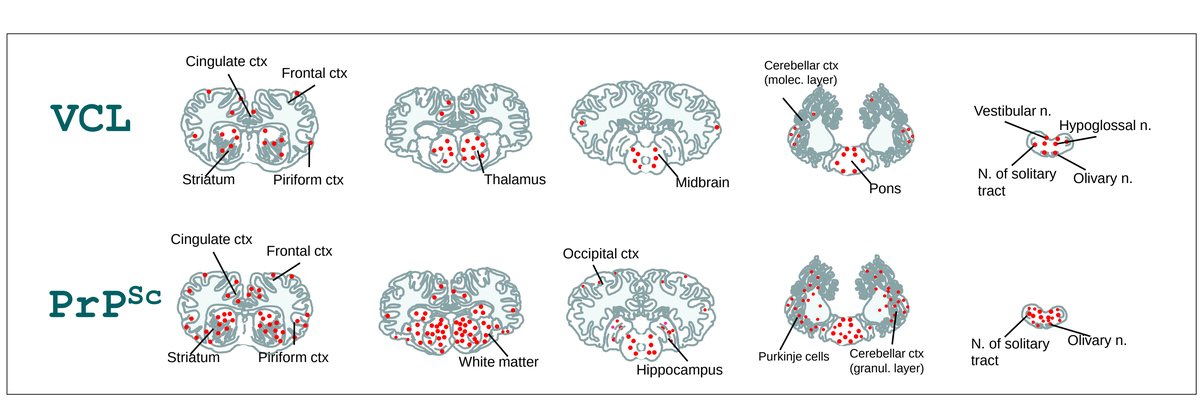

Figure 1. Details of anatomical distribution and severity of vacuolation (VCL) and PrP^{Sc} deposition (PrP^{Sc}) in the dromedary brains examined in this work.

Cortical and subcortical areas

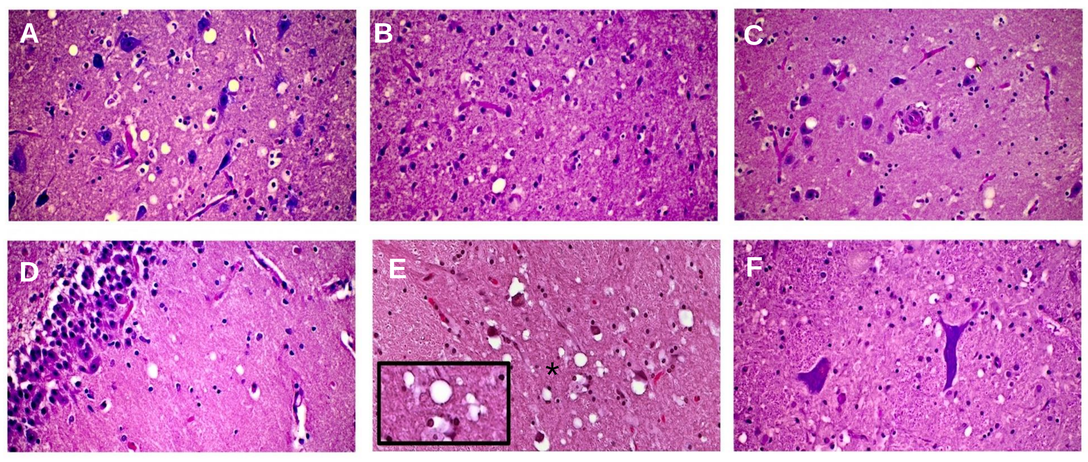

Figure 2. In the grey matter of the cortices, vacuoles were small and medium and confined in the neuropil of the I, II and VI layer (Figure 2A). Rarely confluent vacuoles were observed. White matter showed rare and scattered vacuoles (Figure 2B).

Contrariwise, in basal ganglia, minimal spongiform change of neuropil in either putamen or globus pallidus (lenticular nucleus) was present (Figure 2C). Vacuoles in the hippocampus were preferentially localized in the subiculum, dentate gyrus (Figure 2D) and the hippocampal fimbria, showing slight vacuolation. In the thalamus, moderate spongiform change was mainly observed in ventral and mediodorsal nuclei in which vacuoles involved both neuropil (Figure 2E) and neuronal perikarya, showing homogeneous distribution.

In the midbrain vacuolation was slight present in substantia nigra, oculomotor nucleus and periaqueductal area. The red nucleus (Figure 2F) and external layers of the inferior colliculus showed minimal spongiform change.

Distribution of PrP^{Sc} in the brain

The neuroanatomical distribution and deposition pattern of PrP^{Sc} were evaluated by IHC and Pet-blot, respectively. In general, we found that all areas included in this study were immunolabelled, also where spongiform change was absent. In particular, we found that cortices were less immunolabelled than subcortical areas and caudal brainstem, confirming what was already observed by histopathology. No PrP^{Sc} immunostaining was seen in the CPrD-negative brain.

Cerebral cortex

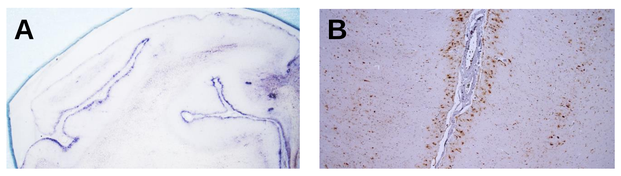

Figure 3. Slight and moderate PrP^{Sc} deposits were observed in prefrontal, frontal, cingulate and piriform cortices, while temporal and parietal cortices were less affected. Irrespective of the intensity of PrP^{Sc} immunolabeling, all positive cortices had the I, V and VI layers involved, while the other layers were more affected in the samples with slight and moderate deposits (Figure 3A and B). White matter was moderately immunolabeled, showing the uneven distribution of PrP^{Sc} deposition (Figure 3A).

Cerebellum

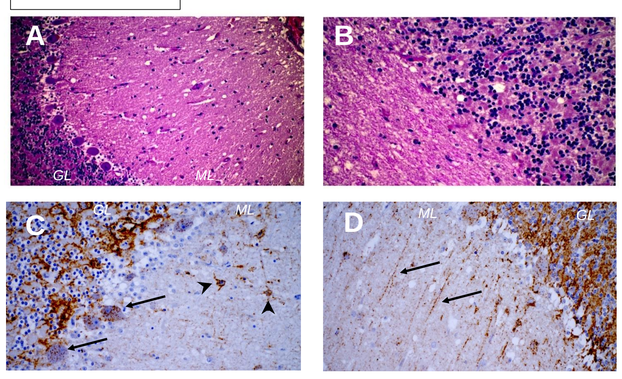

Figure 4. The molecular layer (ML) was positive in all cases, showing small vacuoles from minimal to marked. Purkinje cell bodies were rarely vacuolized (Figure 4A). Spongiosis in the granular layer (GL) was minimal or slight, rarely accompanied by granular loss (Figure 2B).

The molecular layer showed variable PrP^{Sc} immunolabelling with punctate and intra-astrocytic patterns (Figure 4C – arrow heads). Numerous astrocyte projections in the neuropil were also observed (Figure 4D - arrows). Purkinje cells were slightly or moderately immunolabeled, showing fine intraneuronal deposits (Figure 4C - arrows). The granular layer of all cases showed slight and moderate immunolabeling of the extracellular matrix.

Obex

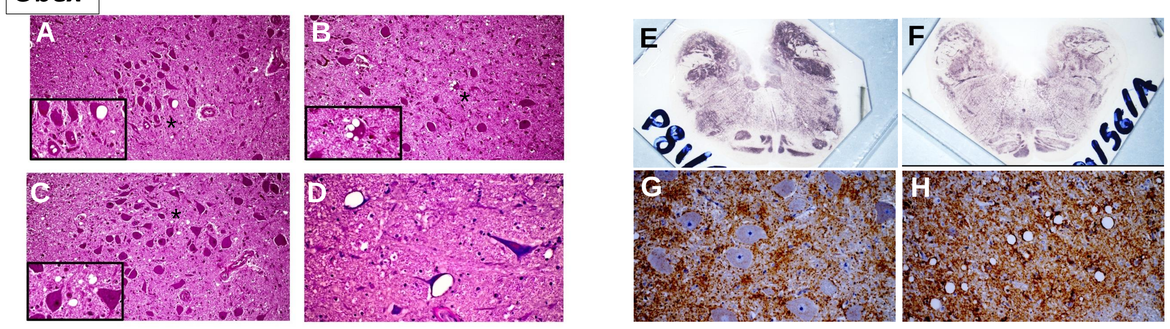

Tables of anatomical distribution and severity of vacuolation (Table 2) and PrP^{Sc} accumulation (Table 3)

Table 2 – Spongiform change in the obex

	#3	#4	#8	#54	#56	#61	#5
Dorsal motor n. of vagus nerve	3	3	3	3	2	3	0
Hypoglossal nucleus	1	2	2	4	2	3	0
Solitary tract n.	2	2	3	3	-	-	0
Lateral cuneate n.	2	2	2	4	3	4	0
Spinal tract n. of trig. nerve	2	3	2	3	2	4	0
Olivary nucleus	3	3	3	4	4	2	0

Table 3 - PrP^{Sc} deposition in the obex

#3	#4	#8	#54	#56	#61	#5
2	2	2	4	3	3	0
2	3	2	4	3	3	0
2	2	2	3	-	-	0
3	3	2	3	3	3	0
3	3	2	3	2	3	0
2	4	3	4	3	4	0

Figure 5. The severity of vacuolation was moderate and marked in the medulla oblongata, in which vacuoles affected both neuropil and neuronal perikarya (Figure 5A-D). As shown in Table 2, we observed spongiform change in all nuclei analyzed (Figure 5A-D).

In general, PrP^{Sc} immunolabeling was more prominent in grey matter, while the white matter was affected by minimal or slight signals (Table 3 and Figure 5E and F). An in-depth analysis of nuclei highlighted slight variability among samples. In particular, we found that case #54 showed the highest labelling (Table 3), with a marked signal of the dorsal motor nucleus of the vagus nerve, and hypoglossal (Figure 5G) and olivary nuclei (Figure 5H).

DISCUSSION AND CONCLUSIONS

Data collected in the present study suggest that the medulla oblongata and sub-cortical areas are the most consistent and appropriate regions of CNS for CPrD diagnosis.

Due to the extensive involvement of brain areas by prion pathology, CPrD is quite similar to that described for classical scrapie of sheep (González et al., 2010; Spiropoulos et al., 2007; Vidal et al., 2009) and CWD of cervids (Williams et al., 1993; Benestad et al., 2018). The immunolabelling observed in both molecular and granular layers of cerebellum of CPrD was reminiscent of what was described for cattle with L-type BSE and atypical scrapie in sheep. Thus, due to the extensive involvement of the cerebellum, this area could be considered another relevant brain region for CPrD diagnosis.

The neuropathological characterization of CPrD in wild-type Algerian dromedaries lays the groundwork for further investigation of cases in dromedaries carrying different genotypes or coming from other Countries.